

**Programmable self-assembly of water-soluble organo-heterometallic cages  $[M_{12}M'_4L_{12}]$  using 3-(3,5-dimethyl-1H-pyrazol-4-yl)pentane-2,4-dione ( $H_2L$ )**

Table of Contents

1. Procedure

Synthesis and physical properties of complexes

2. NMR and MS data

$^1H$  NMR and  $^{13}C$  NMR of all the compounds

Analysis of the NMR spectra

ESI-MS and CSI-MS

3. X-ray diffraction measurement

Crystal structures data

Analysis of the crystal structures

4. References

## Supporting Information

**Materials:** All chemicals and solvents were of reagent grade and were purified according to conventional methods.

**Instrumentation:**  $^1\text{H}$  NMR experiments of all compounds were recorded at 400 MHz on a Bruker Avance III HD 400 spectrometer using tetramethylsilane. ESI-MS and CSI-MS measurements were performed with an JEOL Accu-TOF-4G LC-plus mass spectrometer.

### X-ray Structural Determinations:

X-Ray diffraction data of the crystals of complex  $2 \cdot 12\text{PF}_6^-$  were carried out at 291K using synchrotron radiation ( $\lambda = 0.80010 \text{ \AA}$ ) via the 3W1A in the IHEP with the approval of the Beijing Synchrotron Radiation Facility (BSRF). The diffraction data reduction and integration were performed by the HKL2000 software. Positions of the Pd and Fe atoms and most of the non-hydrogen atoms were found using the direct methods program in the Bruker SHELXTL software. All hydrogen atoms were placed in calculated positions in the final structure refinement. Data for  $\text{C1} \cdot 2\text{PF}_6^-$  and  $1 \cdot 12\text{PF}_6^-$  were collected at 123 K on a Bruker Smart Apex CCD area detector equipped with a graphite monochromated  $\text{MoK}\alpha$  radiation ( $\lambda = 0.71073 \text{ \AA}$ ). The absorption correction for complex was performed using SADABS. The structure was solved by direct methods and refined by employing full-matrix least-squares on  $F^2$  by using the SHELXTL software program and expanded using Fourier techniques.<sup>1-2</sup> All non-H atoms of the complexes were refined with anisotropic thermal parameters. The hydrogen atoms were included in idealized positions. In complexes  $1 \cdot 12\text{PF}_6^-$  and  $2 \cdot 12\text{PF}_6^-$ , the unit cell includes a large region of disordered solvent acetonitrile molecules, which could not be modelled as discrete atomic sites. We employed PLATON/SQUEEZE to calculate the diffraction contribution of the solvent acetonitrile molecules, thereby, to produce a set of solvent-free  $\text{CH}_3\text{CN}$ .

CCDC1524843(C1), 1524844(1) and 1524845(2) contains the supplementary crystallographic data for this paper. These data can be achieved via the Cambridge Crystallographic Data Centre deposit @ccdc.cam.Ac.uk,

<http://www.ccdc.cam.ac.uk/deposit>.

The final residuals along with unit cell, space group, data collection, and refinement parameters are presented in Table S1-S5.

## **Experimental Section:**

### **Synthesis of ligand H<sub>2</sub>L**

Ligand 3-(3,5-dimethyl-1*H*-pyrazol-4-yl)pentane-2,4-dione (**H<sub>2</sub>L**) was synthesized according to a reported procedure with spectroscopic data consistent with the literature<sup>3,4</sup>.

### **Self-assembly of dimetallic corners**

**Synthesis of [(bpy)<sub>2</sub>Pd<sub>2</sub>(HL)<sub>2</sub>](NO<sub>3</sub>)<sub>2</sub> (C1·2NO<sub>3</sub><sup>-</sup>).** **H<sub>2</sub>L** (10.1mg, 0.052mmol) was added to a suspension of bpyPd(NO<sub>3</sub>)<sub>2</sub> (20mg, 0.052mmol) in H<sub>2</sub>O (3ml), and the mixture was stirred for 24 h at room temperature. Then, removing the mixture into 60°C oil-bath for 8 h and the solution became clear. <sup>1</sup>H NMR confirmed the quantitative formation of C1·2NO<sub>3</sub><sup>-</sup>. <sup>1</sup>H NMR (400 MHz, D<sub>2</sub>O, Si(CH<sub>3</sub>)<sub>4</sub> as external standard, 298 K, ppm): 8.55 (d, *J* = 8.0 Hz, 4H, py-H), 8.45 (s, 4H, py-H), 8.24 (d, *J* = 4.0 Hz, 4H, py-H), 7.82 (s, 4H, py-H), 2.37 (s, 12H, pz-H), 2.13 (s, 6H, diketone-H), 1.65 (s, 6H, diketone-H).

The mixture was filtered and a ten-fold excess of KPF<sub>6</sub> was added and vigorous stirring. The yellow precipitation were collected by centrifugation, washed with minimum amount of cold water and dried in vacuum to give C1·2PF<sub>6</sub><sup>-</sup> as yellow solid (23.12 mg, 0.025 mmol, 97.5% yield). ESI-MS (CH<sub>3</sub>CN): *m/z* Calcd for [C1·PF<sub>6</sub><sup>-</sup>]<sup>+</sup> 1056.59 found 1056.94; Calcd for [C1]<sup>2+</sup> 455.82 found 455.99. Elemental analyses calcd (%) for C<sub>40</sub>H<sub>42</sub>F<sub>12</sub>N<sub>8</sub>O<sub>4</sub>P<sub>2</sub>Pd<sub>2</sub>: C, 39.95; H, 3.50; N, 9.32; Found: C, 39.88; H, 3.59; N, 9.28.

**Synthesis of [(dmbpy)<sub>2</sub>Pd<sub>2</sub>(HL)<sub>2</sub>](NO<sub>3</sub>)<sub>2</sub> (C2·2NO<sub>3</sub><sup>-</sup>).** **H<sub>2</sub>L** (9.4 mg, 0.05mmol) was added to a suspension of dmbpyPd(NO<sub>3</sub>)<sub>2</sub> (20.7 mg, 0.05 mmol) in H<sub>2</sub>O (3ml), and the mixture was stirred for 24 h at room temperature. Then, removing the mixture into 60 °C oil-bath for 8 h and the addition of 0.5 ml of acetone to the solution resulted in the suspension liquid became clear immediately. <sup>1</sup>H NMR confirmed the quantitative

formation of  $\mathbf{C2} \cdot 2\text{NO}_3^-$ .  $^1\text{H}$  NMR (400 MHz,  $\text{D}_2\text{O}$ ,  $\text{Si}(\text{CH}_3)_4$  as external standard, 300 K, ppm): 8.55 (d,  $J = 8.0$  Hz, 4H, py-H), 8.45 (s, 4H, py-H), 8.24 (d,  $J = 4.0$  Hz, 4H, py-H), 7.82 (s, 4H, py-H), 2.37 (s, 12H, pz-H), 2.13 (s, 6H, diketone-H), 1.65 (s, 6H, diketone-H).

The mixture was filtered and a ten-fold excess of  $\text{KPF}_6$  was added and vigorous stirring. The yellow precipitation were collected by centrifugation, washed with minimum amount of cold water and dried in vacuum to give  $\mathbf{C2} \cdot 2\text{PF}_6^-$  as yellow solid (23.73 mg, 0.0245 mmol, 98.1% yield). ESI-MS ( $\text{CH}_3\text{CN}$ ):  $m/z$  Calcd for  $[\mathbf{C2} \cdot \text{PF}_6^-]^+$  1112.72 found 1112.99; Calcd for  $[\mathbf{C2}]^{2+}$  483.88 found 484.02. Elemental analyses calcd (%) for  $\text{C}_{44}\text{H}_{50}\text{F}_{12}\text{N}_8\text{O}_4\text{P}_2\text{Pd}_2$ : C, 42.02; H, 4.01; N, 8.91; Found: C, 42.08; H, 4.16; N, 8.93.

#### Self-assembly of hetero-metallic cages

$\{[(\text{bpy})\text{Pd}]_{12}\text{Fe}_4\text{L}_{12}\}(\text{PF}_6)_{12}$  ( $\mathbf{1} \cdot 12\text{PF}_6^-$ ).  $\text{NaHCO}_3$  (8.4 mg, 0.104 mmol) was added to a suspension of  $\mathbf{C1} \cdot 2\text{NO}_3^-$  (23.6 mg, 0.026 mmol) in  $\text{H}_2\text{O}$  (3 ml), and the mixture was stirred for 3 h at room temperature. Then,  $\text{FeCl}_3$  (2.8 mg, 0.017 mmol) was added to the solution and the mixture was stirred for 8 h at 60 °C. The mixture was filtered and a ten-fold excess of  $\text{KPF}_6$  was added and vigorous stirring. The red precipitation were collected by centrifugation, washed with minimum amount of cold water and dried in vacuum to give  $\mathbf{1} \cdot 12\text{PF}_6^-$  as red solid (26.7 mg, 3.62  $\mu\text{mol}$ , 85.2% yield). CSI-MS ( $\text{CH}_3\text{CN}$ ):  $m/z$  Calcd for  $[\mathbf{1} \cdot 9\text{PF}_6^-]^{3+}$  2328.58 found 2328.99; Calcd for  $[\mathbf{1} \cdot 8\text{PF}_6^-]^{4+}$  1710.20 found 1709.76; Calcd for  $[\mathbf{1} \cdot 7\text{PF}_6^-]^{5+}$  1339.17 found 1339.00; Calcd for  $[\mathbf{1} \cdot 6\text{PF}_6^-]^{6+}$  1091.81 found 1091.68. Elemental analyses calcd (%) for  $\text{C}_{240}\text{H}_{240}\text{F}_{72}\text{Fe}_4\text{N}_{48}\text{O}_{24}\text{P}_{12}\text{Pd}_{12}$ : C, 38.81; H, 3.23; N, 9.06; Found: C, 38.58; H, 3.20; N, 8.46.

$\{[(\text{dmbpy})\text{Pd}]_{12}\text{Fe}_4\text{L}_{12}\}(\text{PF}_6)_{12}$  ( $\mathbf{2} \cdot 12\text{PF}_6^-$ ).  $\text{NaHCO}_3$  (8.4 mg, 0.10 mmol) was added to a suspension of  $\mathbf{C2} \cdot 2\text{NO}_3^-$  (24.2 mg, 0.025 mmol) in  $\text{H}_2\text{O}$  (3 ml) and acetone (0.5 ml), and the mixture was stirred for 3 h at room temperature. Then,  $\text{FeCl}_3$  (2.8 mg, 0.017 mmol) was added to the solution and the mixture was stirred for 8 h at 60 °C. The mixture was filtered and a ten-fold excess of  $\text{KPF}_6$  was added and vigorous stirring. The red precipitation were collected by centrifugation, washed with minimum

amount of cold water and dried in vacuum to give  $\mathbf{2} \cdot 12\text{PF}_6^-$  as red solid (27.6 mg, 3.56  $\mu\text{mol}$ , 83.8% yield). CSI-MS ( $\text{CH}_3\text{CN}$ ) :  $m/z$  Calcd for  $[\mathbf{2} \cdot 9\text{PF}_6^-]^{3+}$  2440.79 found 2440.54; Calcd for  $[\mathbf{2} \cdot 8\text{PF}_6^-]^{4+}$  1794.35 found 1794.12; Calcd for  $[\mathbf{2} \cdot 7\text{PF}_6^-]^{5+}$  1406.49 found 1406.12; Calcd for  $[\mathbf{2} \cdot 6\text{PF}_6^-]^{6+}$  1147.92 found 1147.94. Elemental analyses calcd (%) for  $\text{C}_{264}\text{H}_{288}\text{F}_{72}\text{Fe}_4\text{N}_{48}\text{O}_{24}\text{P}_{12}\text{Pd}_{12}$ : C, 40.84; H, 3.71; N, 8.66; Found: C, 40.75; H, 3.73; N, 8.21.

## NMR and MS spectra

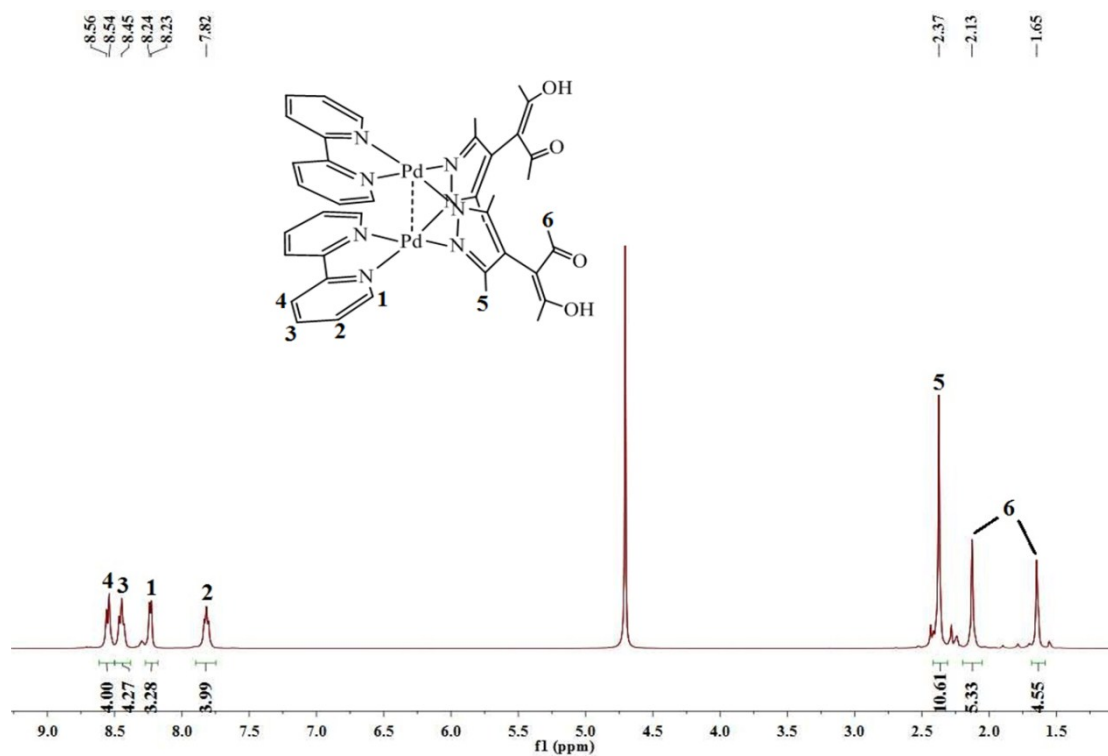


Fig. S1 <sup>1</sup>H NMR (400 MHz, 298 K) spectrum of **C1**·2NO<sub>3</sub><sup>-</sup> in D<sub>2</sub>O.

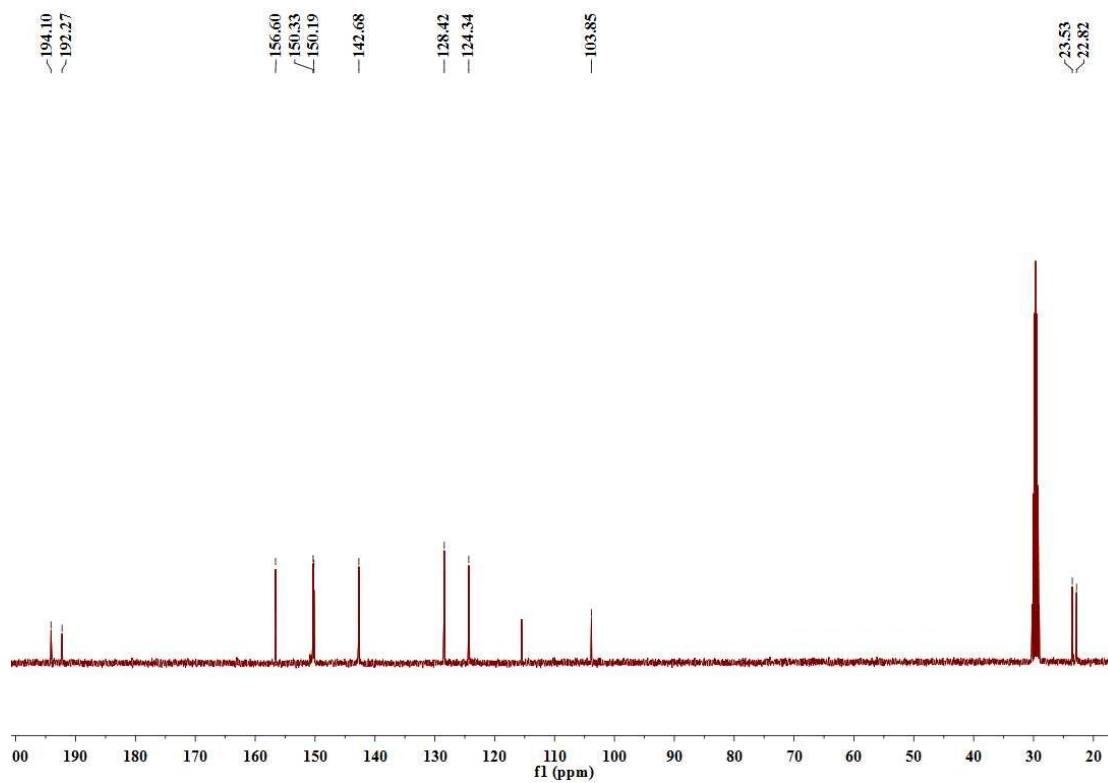


Fig. S2 <sup>13</sup>C NMR (100 MHz, 298 K) spectrum of **C1**·2NO<sub>3</sub><sup>-</sup> in D<sub>2</sub>O.

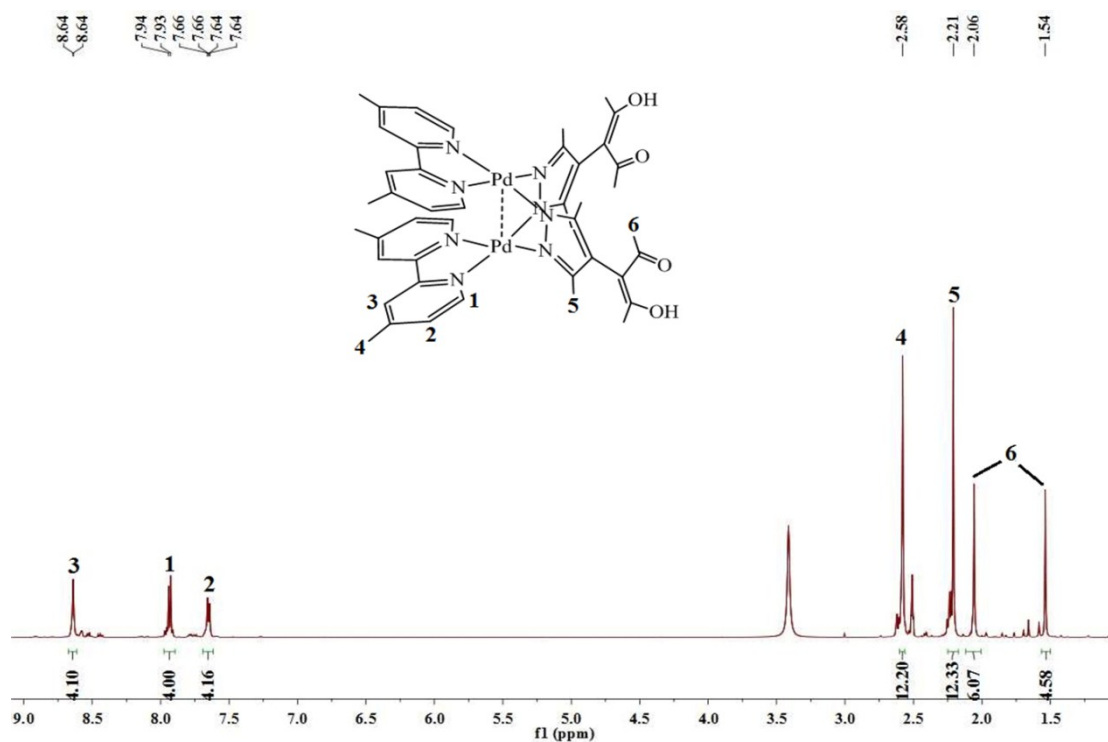


Fig. S3  $^1\text{H}$  NMR (400 MHz, 298 K) spectrum of  $\text{C2} \cdot 2\text{NO}_3^-$  in DMSO.

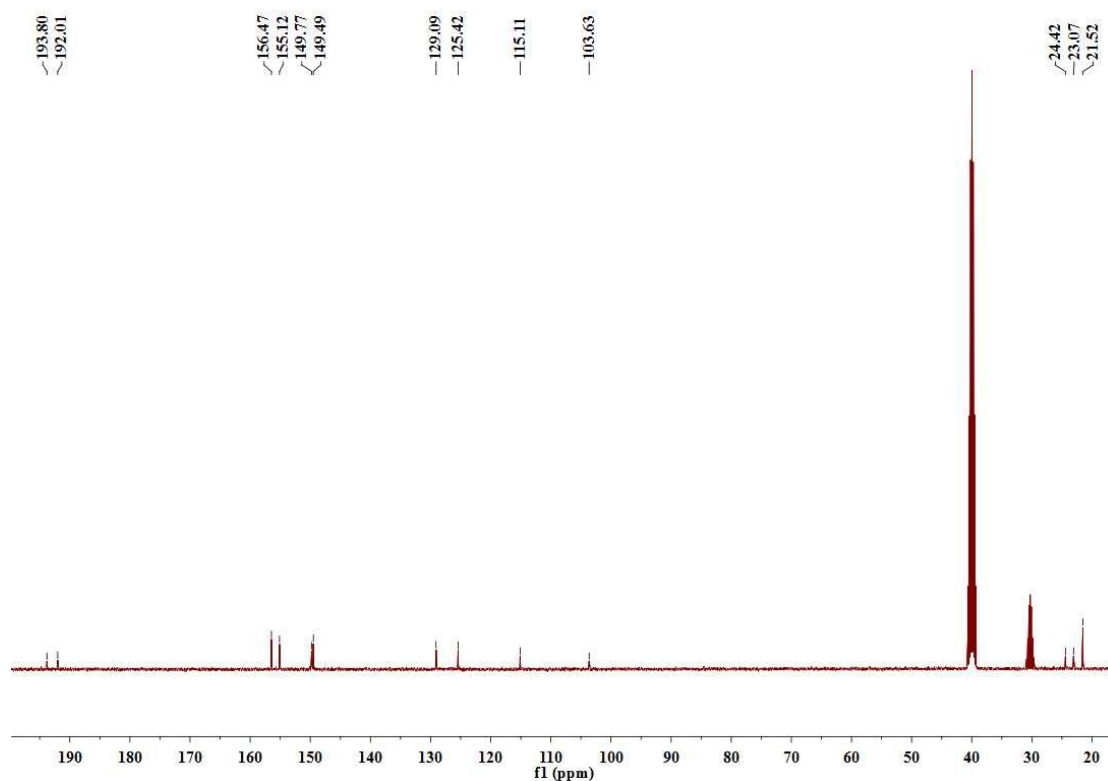
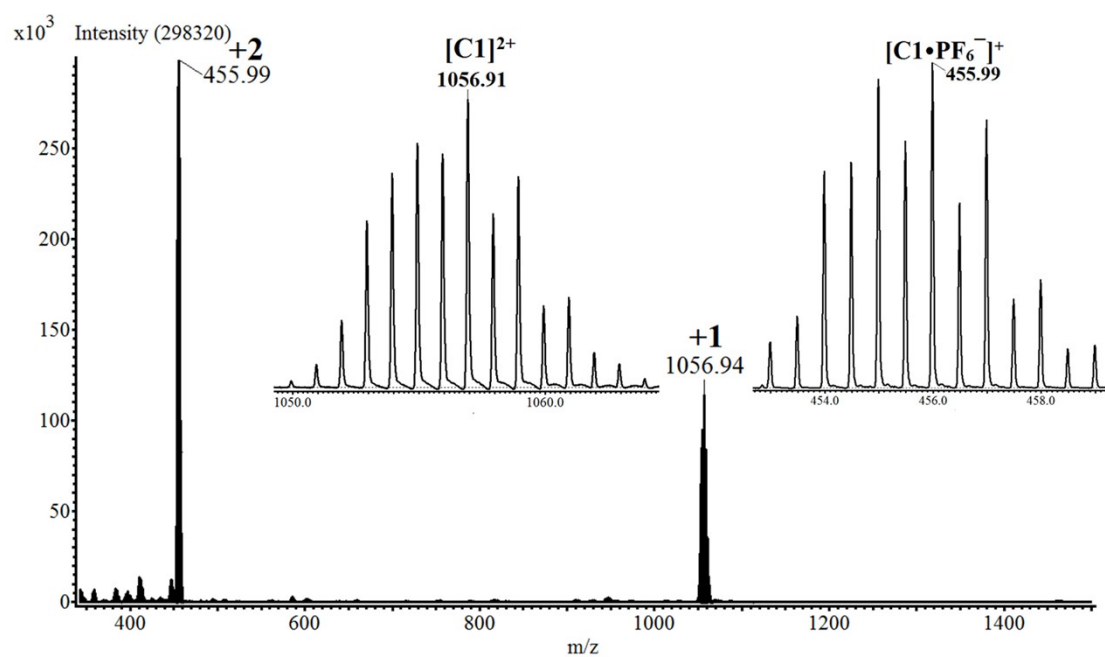


Fig. S4  $^{13}\text{C}$  NMR (100 MHz, 298K) spectrum of  $\text{C2} \cdot 2\text{NO}_3^-$  in DMSO

### Analysis of the NMR spectra

All of  $^1\text{H}$  NMR spectra for the ligand and the self-assembled complexes showed sets of high resolution signals. From the Figure S1 and S3 we could find that the dimetallic clips  $\text{C1}\cdot 2\text{PF}_6^-$  and  $\text{C2}\cdot 2\text{PF}_6^-$  were formed as the pure products and no any other products founded at all in  $\text{D}_2\text{O}$  and DMSO at room temperature. Compared with the pyrazole acetylacetonate ligand, the protons at acetylacetonate methyl of the dimetallic clips had obvious split into two groups. This is due to the rotation of the bond connecting acetylacetonate and pyrazole ligand before assembly, however, the bond would be subject to steric hindrance after assembly, so the chemical environment is different. This also proves the formation of the intermediates.





**Fig. S5** ESI-MS spectrum of  $\text{C1} \cdot 2\text{PF}_6^-$  in acetonitrile. The inset shows the isotopic distribution of the species  $[\text{C1}]^{2+}$  and  $[\text{C1} \cdot \text{PF}_6^-]^+$ .

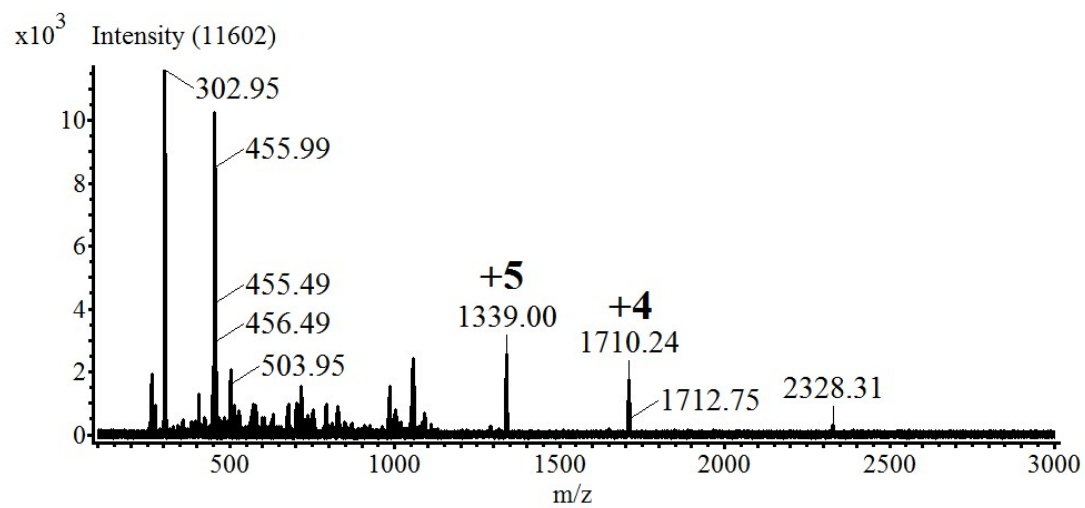


**Fig. S6** ESI-MS spectrum of  $1 \cdot 12\text{PF}_6^-$  in acetonitrile.

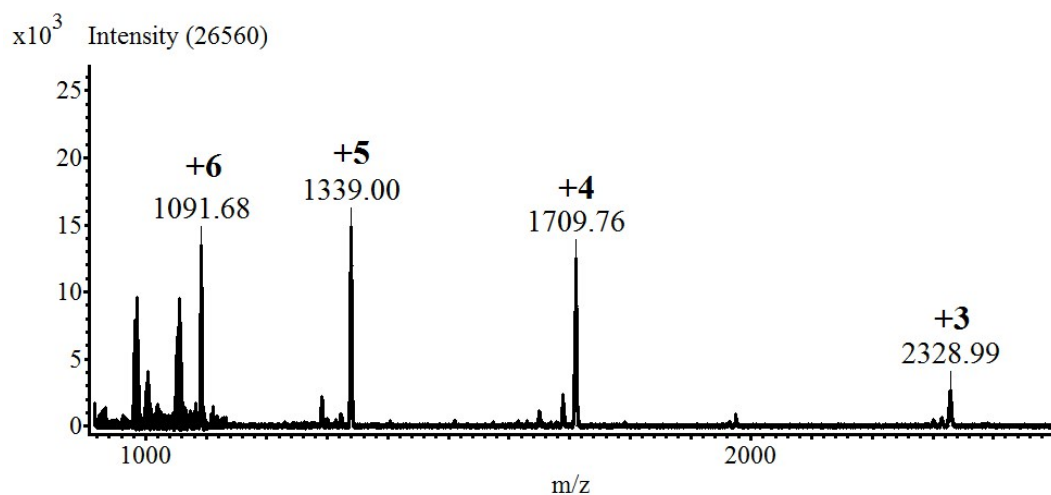


**Fig. S7** CSI-MS spectrum of  $1 \cdot 12PF_6^-$  in acetonitrile.

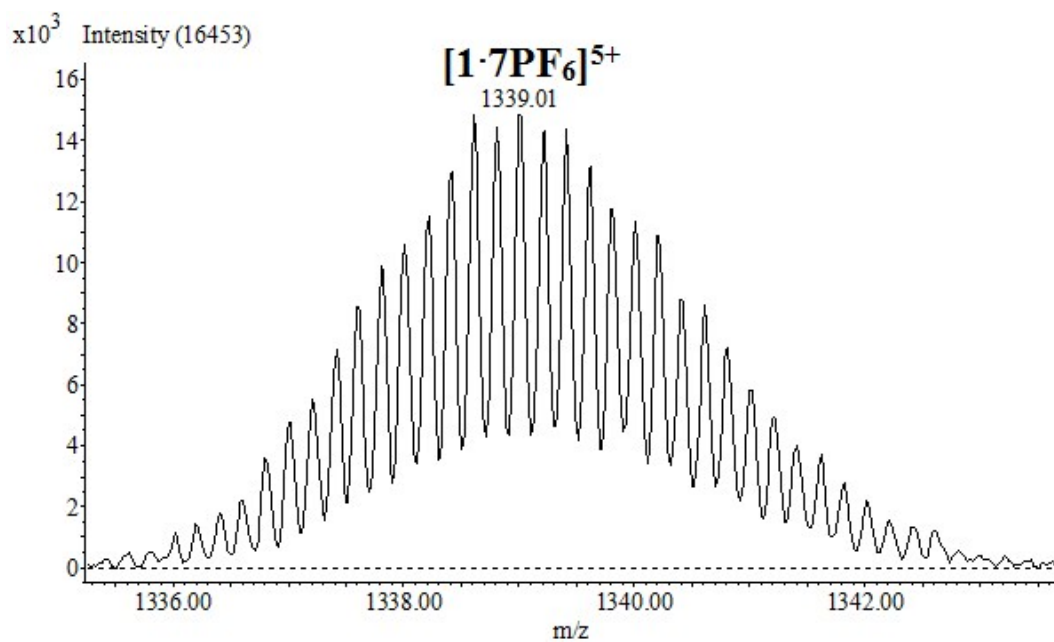


**Fig. S8** The isotopic distribution of the species  $[1 \cdot 7PF_6]^{5+}$ .

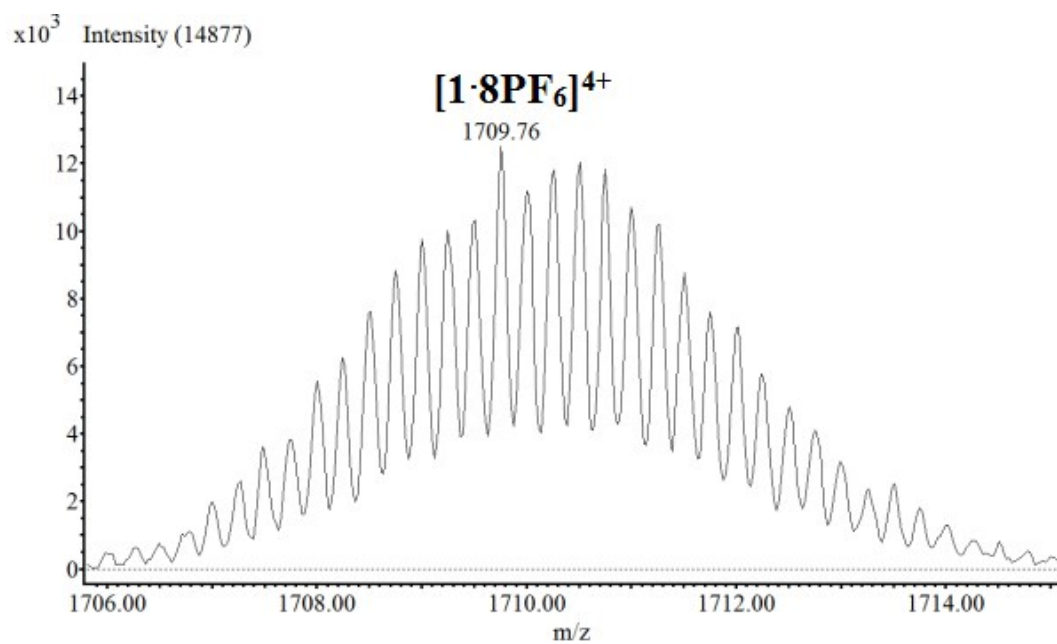


**Fig. S9** The isotopic distribution of the species  $[1 \cdot 8PF_6]^{4+}$ .

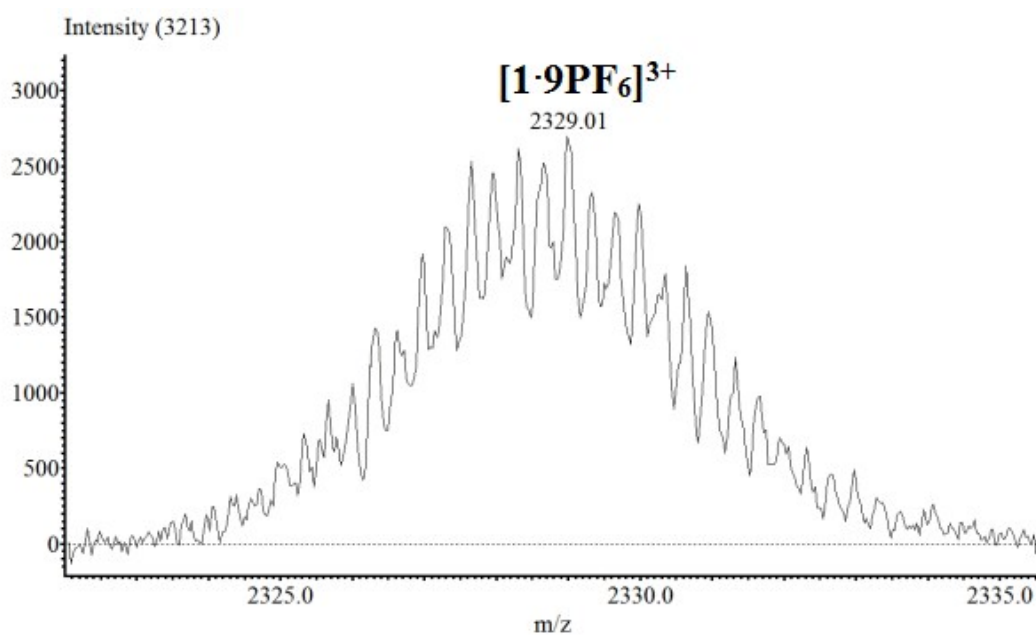


**Fig. S10** The isotopic distribution of the species  $[1 \cdot 9PF_6]^{3+}$ .

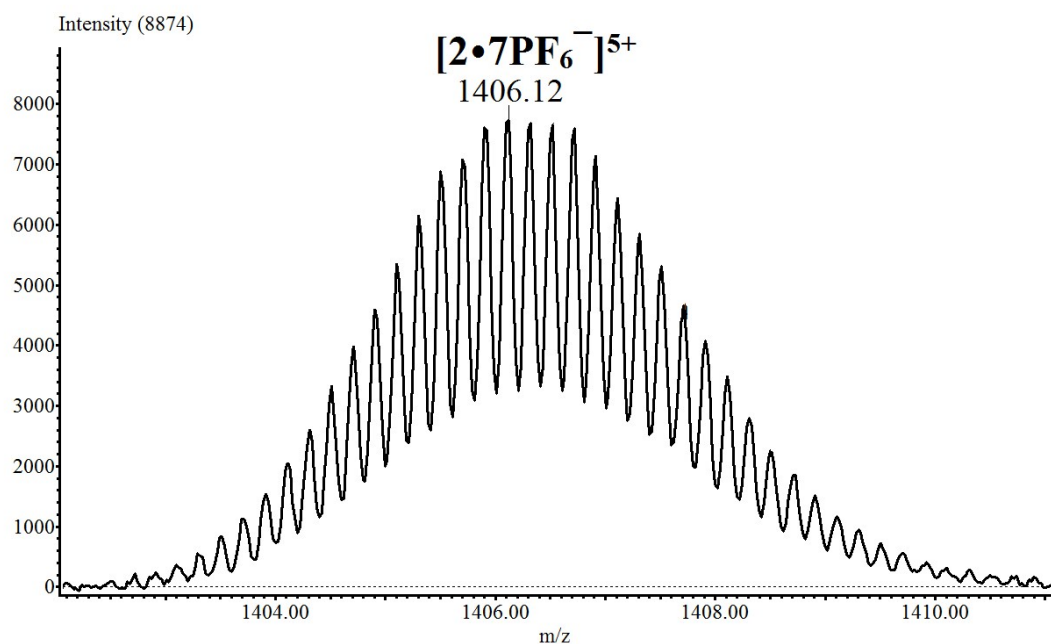


**Fig. S11** The isotopic distribution of the species [2·7PF<sub>6</sub><sup>-</sup>]<sup>5+</sup>.

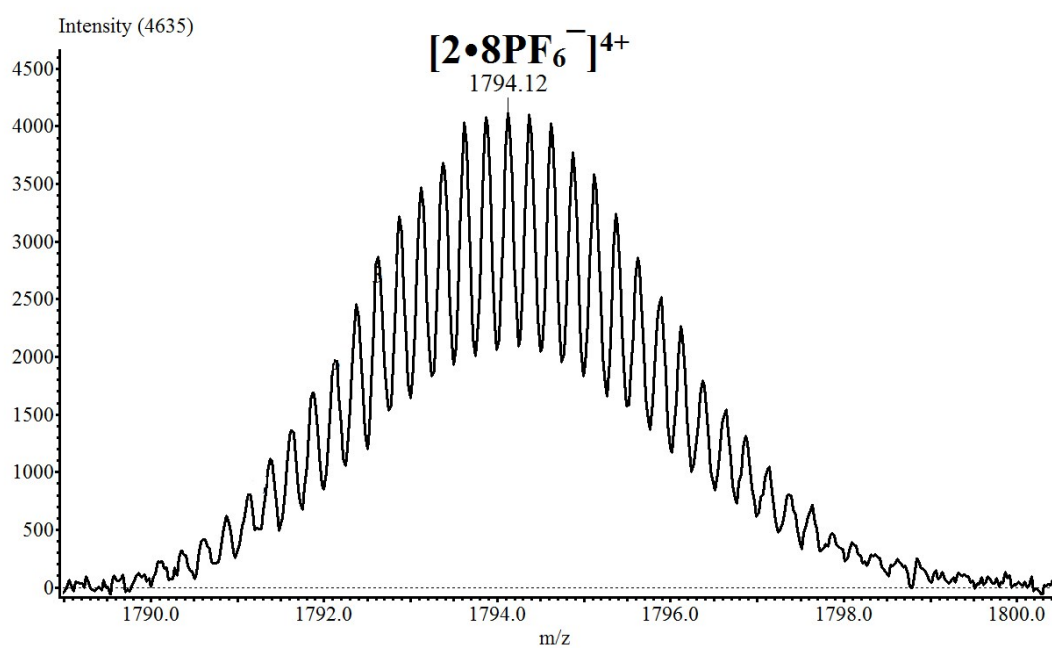


**Fig. S12** The isotopic distribution of the species [2·8PF<sub>6</sub><sup>-</sup>]<sup>4+</sup>.

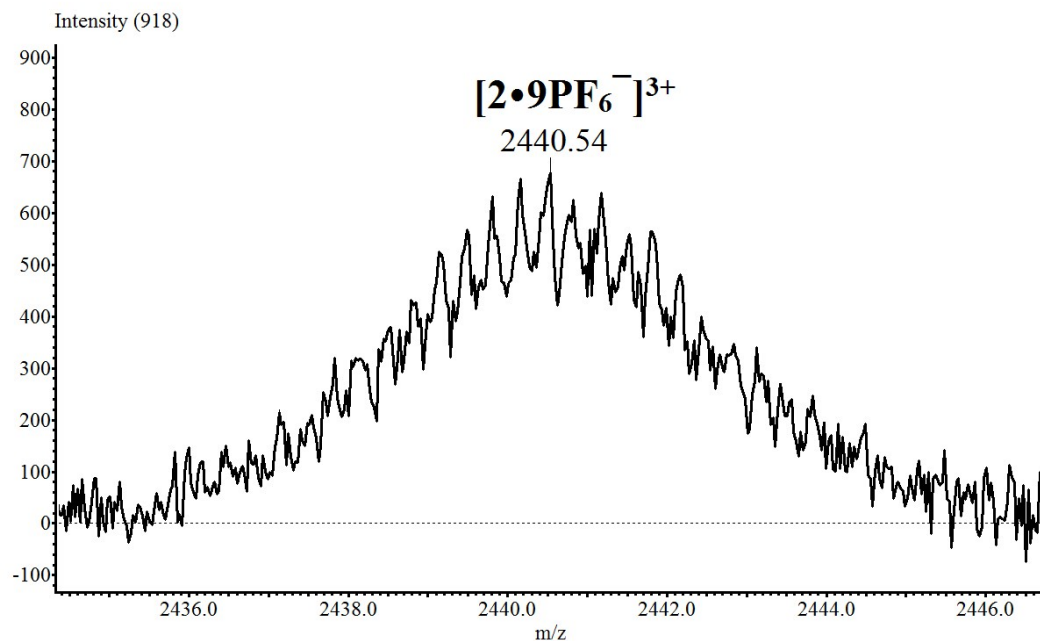


**Fig. S13** The isotopic distribution of the species  $[2 \cdot 9PF_6]^{3+}$ .

#### X-ray diffraction measurement

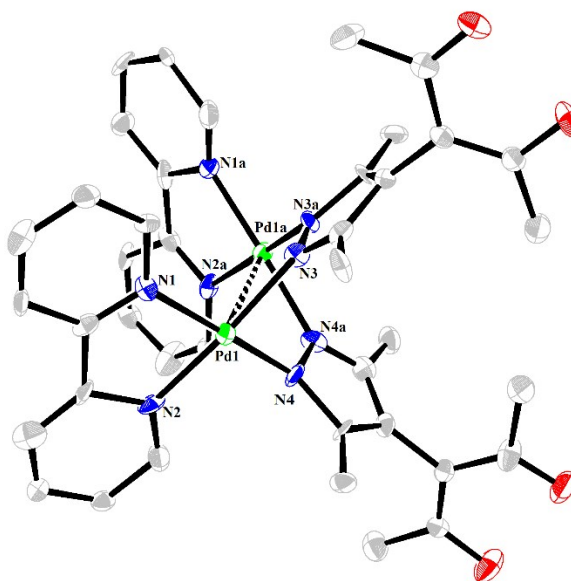


**Fig. S14** ORTEP diagram of the molecular structure of  $C1 \cdot 2PF_6^-$ . Thermal ellipsoids are shown at the 30% probability level. Counter ions and solvent molecules are omitted for clarity.

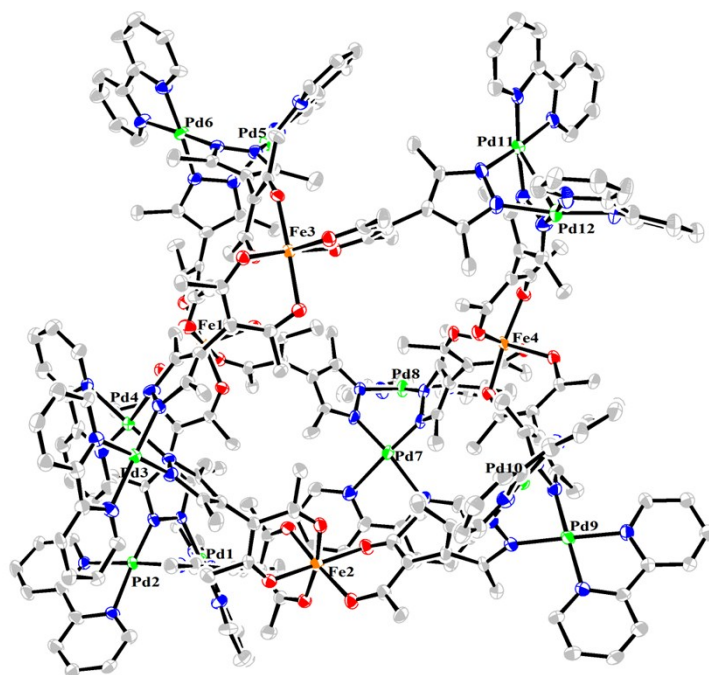


**Fig. S15** ORTEP diagram of the molecular structure of **1**•12PF<sub>6</sub><sup>−</sup>. Thermal ellipsoids are shown at the 30% probability level. Counter ions and solvent molecules are omitted for clarity.

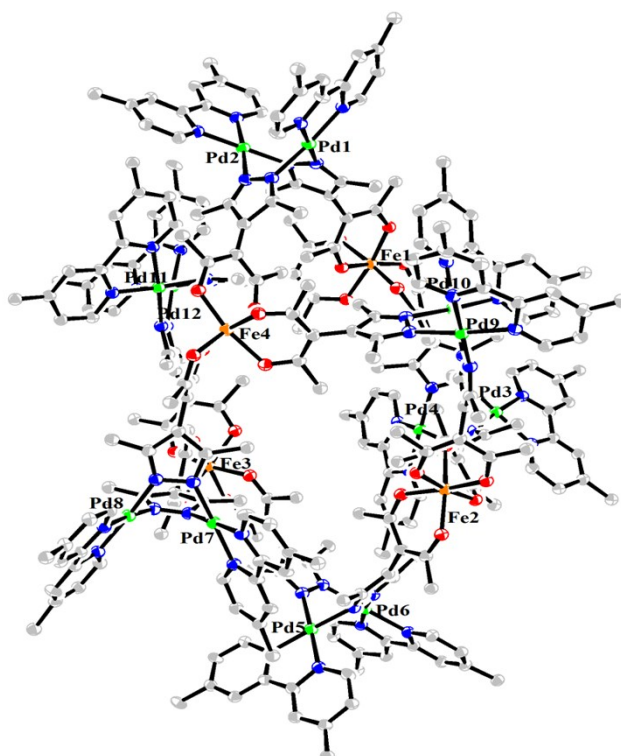


**Fig. S16** ORTEP diagram of the molecular structure of **2**•12PF<sub>6</sub><sup>−</sup>. Thermal ellipsoids are shown at the 30% probability level. Counter ions and solvent molecules are omitted for clarity.

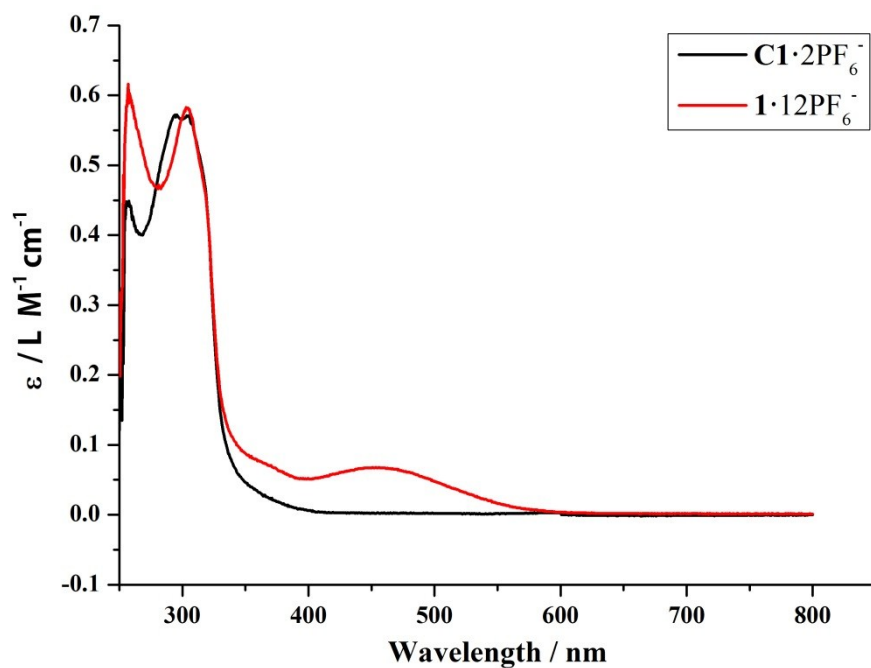


**Fig. S17** UV-vis absorption spectra of compound **C1·2PF<sub>6</sub><sup>-</sup>** and **1·12PF<sub>6</sub><sup>-</sup>** ( $1 \times 10^{-5}$  M) in CH<sub>3</sub>CN at 25 °C (black, **C1·2PF<sub>6</sub><sup>-</sup>**; red, compound **1·12PF<sub>6</sub><sup>-</sup>**).

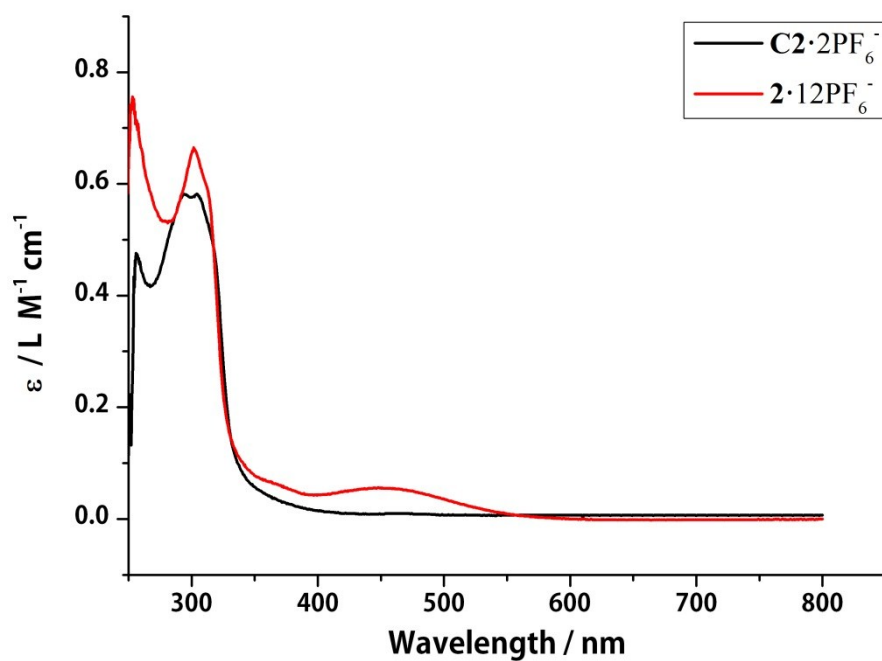


**Fig. S18** UV-vis spectrum of compound **C2·2PF<sub>6</sub><sup>-</sup>** and **2·12PF<sub>6</sub><sup>-</sup>** ( $1 \times 10^{-5}$  M) in CH<sub>3</sub>CN at 25 °C (black, compound **C2·2PF<sub>6</sub><sup>-</sup>**; red, compound **2·12PF<sub>6</sub><sup>-</sup>**)

**Table S1.** Crystallographic data for complexes **C1**·2PF<sub>6</sub><sup>−</sup>, **1**·12PF<sub>6</sub><sup>−</sup> and **2**·12PF<sub>6</sub><sup>−</sup>.

	<b>C1</b> ·2PF <sub>6</sub> <sup>−</sup>	<b>1</b> ·12PF <sub>6</sub> <sup>−</sup>	<b>2</b> ·12PF <sub>6</sub> <sup>−</sup>
Formula	C <sub>40</sub> H <sub>42</sub> F <sub>12</sub> N <sub>8</sub> O <sub>4</sub> P <sub>2</sub> Pd <sub>2</sub>	C <sub>240</sub> H <sub>240</sub> F <sub>72</sub> Fe <sub>4</sub> N <sub>48</sub> O <sub>24</sub> P <sub>12</sub> Pd <sub>12</sub> · 8(CH <sub>3</sub> CN)	C <sub>264</sub> H <sub>288</sub> F <sub>72</sub> Fe <sub>4</sub> N <sub>48</sub> O <sub>24</sub> P <sub>12</sub> Pd <sub>12</sub> · 14(CH <sub>3</sub> CN)
FW	1201.55	7749.02	8831.98
crystal system	orthorhombic	Triclinic	Triclinics
space group	Pnma	P-1	P-1
a [Å]	18.797(4)	25.0517(12)	25.6021(15)
b [Å]	18.398(4)	32.2634(14)	26.9162(12)
c [Å]	13.758(3)	35.368(2)	36.6641(13)
α [°]	90	108.9680(10)	68.991(2)
β [°]	90	101.156(2)	73.112(2)
γ [°]	90	108.3630(10)	64.351(3)
V [Å <sup>3</sup> ]	4757.9(18)	24223(2)	20985.3(18)
Z	4	2	2
ρ <sub>calcd</sub> , [g/cm <sup>−3</sup> ]	1.677	1.017	1.267
μ [mm <sup>−1</sup> ]	0.919	0.657	1.039
F(000)	2400	7384	7768
2θ <sub>max</sub> [°]	50.00	54.00	62.52
no. unique data	4209	105551	93235
Parameters	337	3757	3991
GOF [F <sup>2</sup> ] <sup>a</sup>	1.061	0.794	1.010
R[F <sup>2</sup> >2σ(F <sup>2</sup> )]	0.0327	0.0408	0.0511
wR[F <sup>2</sup> ] <sup>b</sup>	0.0892	0.1028	0.1235

**Platon-squeeze details and solvents assignment for cage 1:**

The crystallography revealed that cage **1** crystallized in lower symmetry space group p-1 and two formula units existed in one cell. Based on the data refined using the platon-squeeze program, each unit has a formula of [C<sub>264</sub>H<sub>288</sub>Fe<sub>4</sub>N<sub>48</sub>O<sub>24</sub>Pd<sub>12</sub>](PF<sub>6</sub>)<sub>12</sub>, as well one void of 11674 Å<sup>3</sup>(377 electrons) located in per unit cell. This residual electron density was assigned to ~17 molecules of the acetonitrile solvent [377=22×17.15]. Due to there are two formula units in one cell, it's possible that the formula unit includes ~8 (17/2=8.5) acetonitrile molecules. On the basis of these results, these solvent molecules were include in the sum formula, formula weight and calculated density, respectively. The tentative formula for cage **1** is [C<sub>240</sub>H<sub>240</sub>Fe<sub>4</sub>N<sub>48</sub>O<sub>24</sub>Pd<sub>12</sub>](PF<sub>6</sub>)<sub>12</sub> (CH<sub>3</sub>CN)<sub>8</sub>.

platon\_squeeze\_void\_nr

platon\_squeeze\_void\_average\_x

platon\_squeeze\_void\_average\_y

platon\_squeeze\_void\_average\_z



```

platon_squeeze_void_volume
platon_squeeze_void_count_electrons
platon_squeeze_void_content
1 0.700 0.053 0.321 11674 377 '17 MeCN'
platon_squeeze_void_probe_radius 1.20
The sum and moiety formulae should be adjusted accordingly:
chemical_formula_moiety
'C240 H240 Fe4 N48 O24 Pd12, 12(F6P) [ 8 MeCN (squeezed)]'
chemical_formula_sum
'C256 H264 F72 Fe4 N56 O24 P12 Pd12 [ solvent]'

```

### Platon-squeeze details and solvents assignment for cage 2:

The refined crystal structure indicated that cage 2 crystallized in lower symmetry space group p-1 with two formula in per cell. When we used the squeeze to refine this crystal data to solve all solvent molecules last time, the squeezed data reveals a formula  $[C_{264}H_{288}Fe_4N_{48}O_{24}Pd_{12}](PF_6)_{12}$ , as well a void of 7373 Å<sup>3</sup>(604 electrons) located in per unit cell. This residual electron density was assigned to ~28 molecules of the acetonitrile solvent  $[604 = 22 \times 27.45]$ . Due to there are two formula units in one cell, it's possible that the formula unit includes 14 ( $28 / 2 = 14$ ) acetonitrile molecules.

After we refine this data of cage 2 again, there are 12 CH<sub>3</sub>CN revealed in very well ordered within the cage structure in per cell by difference fourier diagram. The squeeze data reveals a formula  $[C_{264}H_{288}Fe_4N_{48}O_{24}Pd_{12}](PF_6)_{12}(CH_3CN)_6$ , and a void of 6148 Å<sup>3</sup>(474 electrons) located in per cell. This residual electron density was assigned to 22 molecules of the acetonitrile solvent  $[474 = 22 \times 21.54]$  in per cell. Due to there are two formula units in one cell, that the formula unit includes about 7–13 acetonitrile molecules taking account of 30% error ( $22 / 2 \approx 10$ ). According to the number of solvent molecules from the squeezed data last time, we have reason to guess there are about 8 molecules of acetonitrile solvent that are more precise than the number of 10 we calculated according to the residual electron density. On the basis of these results, these solvent molecules were include in the sum formula, formula weight and calculated density, respectively. So, the tentative formula for cage 2 is  $[C_{264}H_{288}Fe_4N_{48}O_{24}Pd_{12}](PF_6)_{12}(CH_3CN)_{14}$ .

```

platon_squeeze_void_nr
platon_squeeze_void_nr
platon_squeeze_void_average_x
platon_squeeze_void_average_y
platon_squeeze_void_average_z

```

platon_squeeze_void_volume					
platon_squeeze_void_count_electrons					
platon_squeeze_void_content					
1	0.007	-0.007	0.000	7373	604 '16CH3CN'
2	0.767	0.416	0.193	13	-1 ''
3	0.233	0.584	0.807	12	-1 ''
chemical_formula_moiety					
'C264 H288 Fe4 N48 O24 Pd12, 12(F6 P),14(MeCN)'					
chemical_formula_sum					
'C292 H330 F72 Fe4 N62 O24 P12 Pd12'					
chemical_formula_weight				8331.98	

**Table S2.** Selected bond distances (Å) for complex **C1**·2PF<sub>6</sub><sup>−</sup>, **1**·12PF<sub>6</sub><sup>−</sup> and **2**·12PF<sub>6</sub><sup>−</sup>.

C1·2PF <sub>6</sub> <sup>−</sup>		1·12PF <sub>6</sub> <sup>−</sup>		2·12PF <sub>6</sub> <sup>−</sup>	
Pd1-Pd1a	3.1357(8)	Pd1-Pd2	3.2323(4)	Pd1-Pd2	3.2388(4)
		Pd3-Pd4	3.2851(4)	Pd3-Pd4	3.2475(4)
		Pd5-Pd6	3.2197(4)	Pd5-Pd6	3.2513(4)
		Pd7-Pd8	3.2500(4)	Pd7-Pd8	3.2665(4)
		Pd9-Pd10	3.2027(4)	Pd9-Pd10	3.1346(4)
		Pd11-Pd12	3.1826(4)	Pd11-Pd12	3.2597(4)
		Fe1-Fe2	11.3165	Fe1-Fe2	11.7086
		Fe1-Fe3	11.3790	Fe1-Fe3	11.2921
		Fe1-Fe4	11.4655	Fe1-Fe4	11.2536

Fe2-Fe3	11.9849	Fe2-Fe3	11.3407
Fe2-Fe4	11.0181	Fe2-Fe4	11.4311
Fe3-Fe4	10.7871	Fe3-Fe4	11.7767

**Table S3.** Selected bond distances (Å) for complex **C1**·2PF<sub>6</sub><sup>−</sup>.

Bond Dist. (Å)		Bond Dist. (Å)	
Pd1-N1	2.025(2)	Pd1-N2	2.035(2)
Pd1-N3	2.012(2)	Pd1-N4	2.011(2)

**Table S4.** Selected bond distances (Å) for complex **1**·12PF<sub>6</sub><sup>−</sup>.

Bond Dist. (Å)		Bond Dist. (Å)	
Pd1-N1	1.954(3)	Pd1-N2	2.093(3)
Pd1-N25	1.895(2)	Pd1-N27	1.934(3)
Pd2-N3	2.164(2)	Pd2-N4	1.992(2)
Pd2-N26	1.926(2)	Pd2-N28	1.922(2)
Pd3-N5	2.064(2)	Pd3-N6	1.932(3)
Pd3-N29	1.939(3)	Pd3-N31	1.951(2)
Pd4-N7	2.022(2)	Pd4-N8	1.966(3)
Pd4-N30	1.921(2)	Pd4-N32	1.940(3)
Pd5-N9	1.996(3)	Pd5-N10	1.974(3)
Pd5-N33	1.943(3)	Pd5-N35	1.915(3)
Pd6-N11	2.036(3)	Pd6-N12	1.971(3)
Pd6-N34	2.043(3)	Pd6-N36	1.915(3)

---

Pd7-N13	2.304(3)	Pd7-N14	2.345(3)
Pd7-N37	1.878(3)	Pd7-N39	1.928(3)
Pd8-N15	2.435(3)	Pd8-N16	2.312(3)
Pd8-N38	1.903(3)	Pd8-N40	1.949(3)
Pd9-N17	1.962(3)	Pd9-N18	2.023(3)
Pd9-N41	1.963(3)	Pd9-N43	1.962(3)
Pd10-N19	2.017(3)	Pd10-N20	2.055(3)
Pd10-N42	1.963(3)	Pd10-N44	1.988(3)
Pd11-N21	1.946(3)	Pd11-N22	2.070(3)
Pd11-N45	1.993(3)	Pd11-N47	1.884(3)
Pd12-N23	1.964(3)	Pd12-N24	1.990(3)
Pd12-N46	1.996(3)	Pd12-N48	1.983(3)
Fe1-O1	2.001(2)	Fe1-O2	1.968(2)
Fe1-O3	1.946(2)	Fe1-O4	1.994(2)
Fe1-O5	1.995(2)	Fe1-O6	2.006(2)
Fe2-O7	2.000(2)	Fe2-O8	2.012(2)
Fe2-O9	1.987(2)	Fe2-O10	1.997(2)
Fe2-O11	2.059(2)	Fe2-O12	2.001(2)
Fe3-O13	1.999(2)	Fe3-O14	2.146(2)
Fe3-O15	2.0176(19)	Fe3-O16	2.015(2)
Fe3-O17	1.991(2)	Fe3-O18	1.995(2)

---

Fe4-O19	2.007(2)	Fe4-O20	2.032(2)
Fe4-O21	2.013(2)	Fe4-O22	2.015(2)
Fe4-O23	2.013(2)	Fe4-O24	2.009(2)

**Table S5.** Selected bond distances (Å) for complex **2**·12PF<sub>6</sub><sup>−</sup>.

	Bond Dist. (Å)		Bond Dist. (Å)
Pd1-N1	2.052(2)	Pd1-N2	2.000(2)
Pd1-N25	2.075(3)	Pd1-N27	2.033(2)
Pd2-N3	2.033(2)	Pd2-N4	1.980(2)
Pd2-N26	2.045(2)	Pd2-N28	2.021(2)
Pd3-N5	2.049(2)	Pd3-N6	2.030(3)
Pd3-N29	2.011(2)	Pd3-N31	2.028(2)
Pd4-N7	2.027(2)	Pd4-N8	1.997(2)
Pd4-N30	2.026(2)	Pd4-N32	2.085(2)
Pd5-N9	1.995(2)	Pd5-N10	2.049(2)
Pd5-N33	2.075(2)	Pd5-N35	1.996(2)
Pd6-N11	2.055(2)	Pd6-N12	2.023(2)
Pd6-N34	2.020(2)	Pd6-N36	2.039(2)
Pd7-N13	2.019(2)	Pd7-N14	2.021(2)
Pd7-N46	2.065(2)	Pd7-N48	2.064(2)
Pd8-N15	2.039(2)	Pd8-N16	2.013(2)
Pd8-N45	2.014(2)	Pd8-N47	1.996(2)

---

Pd9-N17	2.101(3)	Pd9-N18	2.031(2)
Pd9-N37	2.068(3)	Pd9-N39	1.997(2)
Pd10-N19	2.000(3)	Pd10-N20	2.009(2)
Pd10-N38	2.104(3)	Pd10-N40	2.050(2)
Pd11-N21	2.041(2)	Pd11-N22	2.036(3)
Pd11-N41	1.999(2)	Pd11-N43	2.077(3)
Pd12-N23	2.022(3)	Pd12-N24	1.945(2)
Pd12-N42	2.064(2)	Pd12-N44	2.078(2)
Fe1-O1	2.003(2)	Fe1-O2	1.978(2)
Fe1-O3	1.777(2)	Fe1-O4	2.000(2)
Fe1-O5	1.992(2)	Fe1-O6	2.001(2)
Fe2-O7	2.032(2)	Fe2-O8	2.048(2)
Fe2-O9	2.009(2)	Fe2-O10	2.022(2)
Fe2-O11	2.017(2)	Fe2-O12	1.990(2)
Fe3-O13	2.031(2)	Fe3-O14	2.052(2)
Fe3-O15	2.029(2)	Fe3-O16	2.003(2)
Fe3-O17	2.073(2)	Fe3-O18	2.018(2)
Fe4-O19	1.970(2)	Fe4-O20	2.052(2)
Fe4-O21	1.958(2)	Fe4-O22	2.037(2)
Fe4-O23	2.009(2)	Fe4-O24	2.064(2)

---

## Reference

- (1) Sheldrick, G. M. SHELXS-97 (Univ. Göttingen, 1990).
- (2) Sheldrick, G. M. SHELXL-97 (Univ. Göttingen, 1997).
- (3) Mosby, W. L. *Journal of the Chemical Society*. 1957, 3997-4003.
- (4) Charles, Robert G. *Organic Syntheses*. 1959, **39**, 61-63.